On the electrochemical etching of tips for scanning tunneling microscopy

J. P. Ibe, P. P. Bey, S. L. Brandow, R. A. Brizzolara, N. A. Burnham, D. P. DiLella, K. P. Lee, C. R. K. Marrian, and R. J. Colton

Citation: Journal of Vacuum Science & Technology A **8**, 3570 (1990); doi: 10.1116/1.576509
View online: https://doi.org/10.1116/1.576509
View Table of Contents: http://avs.scitation.org/toc/jva/8/4
Published by the American Vacuum Society

On the electrochemical etching of tips for scanning tunneling microscopy

J. P. Ibe,[a] P. P. Bey, Jr., S. L. Brandow, R. A. Brizzolara, N. A. Burnham, D. P. DiLella, K. P. Lee,[b] C. R. K. Marrian,[c] and R. J. Colton
Surface Chemistry Branch, Code 6177, Naval Research Laboratory, Washington, DC 20375-5000

(Received 26 January 1990; accepted 27 February 1990)

The sharpness of tips used in scanning tunneling microscopy (STM) is one factor which affects the resolution of the STM image. In this paper, we report on a direct-current (dc) drop-off electrochemical etching procedure used to sharpen tips for STM. The shape of the tip is dependent on the meniscus which surrounds the wire at the air–electrolyte interface. The sharpness of the tip is related to the tensile strength of the wire and how quickly the electrochemical reaction can be stopped once the wire breaks. We have found that the cutoff time of the etch circuit has a significant effect on the radius of curvature and cone angle of the etched tip; i.e., the faster the cutoff time, the sharper the tip. We have constructed an etching circuit with a minimum cut-off time of 500 ns which uses two fast metal–oxide semiconductor field effect transistors (MOSFET) and a high-speed comparator. The radius of curvature of the tips can be varied from approximately 20 to greater than 300 nm by increasing the cutoff time of the circuit.

I. INTRODUCTION

Scanning tunneling microscopy (STM) is based on the phenomenon that electrons can tunnel across the potential barrier established when two electrodes, in this case a sharp tip and a conducting or semiconducting surface, approach each other under appropriate bias to less than a nanometer.[1,2] The unique sensitivity of STM stems from the exponential dependence of the measured tunneling current on tip-sample separation. The sharpness of the tip is one factor which affects the resolution of the STM image.[3–5]

STM tips are typically fabricated from metal wires of tungsten (W), platinum–iridium (Pt–Ir), or gold (Au) and sharpened by grinding,[1] cutting with a wire cutter or razor blade,[6] "controlled" crashing,[7] field emission/evaporation,[8–10] ion milling,[11,12] fracture,[13] or electrochemical polishing/etching.[14–16] The goal is to produce a sharp metal tip with a low-aspect ratio (tip length/tip shank) to minimize flexural vibrations. Ideally, the tip should be atomically sharp; but in practice, many of the above methods produce a tip with a rather ragged end that consists of several asperities, with the one closest to the surface responsible for tunneling. Atomically sharp tips have been prepared by field evaporation and characterized by field ion microscopy (FIM).[17–21] Kuk *et al.*[18,19] found a direct correlation between the size of the tip and the measured corrugation of Au (100) and (110) surfaces. However, most of us do not use FIM to prepare tips, but rely on luck or some seemingly reproducible method such as electrochemical etching to produce reasonably sharp tips.

Tips used in FIM are in fact usually prepared by electrochemical polishing or etching procedures[22–28] used to thin specimens for transmission electron microscopy. The goal for FIM tip production is not to produce atomically sharp tips but to produce tips that are free of strain or deformation in order to study the atomic structure of the tip material. The etching recipes used to make STM tips are derived from the FIM procedures.

The electrochemical etching procedure usually involves the anodic dissolution of the metal electrode. There are two ways in which this can be done: an alternating-current (ac) etch or a direct-current (dc) etch according to the applied potential. Each procedure gives a different tip shape; the ac etched tips have a conical shape and much larger cone angles than the dc etched tips. The dc etched tips, on the other hand, have the shape of a hyperboloid, are much sharper than ac etched tips and are preferable for high resolution STM imaging. In STM, dc etched tips are usually prepared by the dc drop-off method in which etching occurs at the air/electrolyte interface causing the portion of wire in solution to "drop off" when its weight exceeds the tensile strength of the etched or necked down region of the wire. This presumably leaves a ragged edge of work hardened asperities at the very end of the tip where the fracture occurs. These small asperities decrease the effective radius of curvature of the tunneling tip for high-resolution imaging.

It should be realized however that placing the tungsten tip in an aqueous solution, or for that matter, exposing it to air, results in the formation of a surface oxide (usually WO_3). In order to lower the noise level in STM images, this oxide must be removed.[7–12] As a result, the microstructure at the end of the tip may be altered during the cleaning procedure. Hence, the electrochemical etching procedure described here is used predominately to generate the desired tip shape, while the subsequent cleaning procedure will determine the ultimate performance of the tip.[10]

The dc drop-off method will produce, in effect, two tips simultaneously: the part below the air/electrolyte interface that drops off and the part above the interface. Bryant *et al.*[14] use the lower end stating that the desired asperities remain intact since the etching stops as soon as the lower end drops off. The upper part, however, will continue to etch as long as it remains in the electrolyte under an applied potential. In this study, we have examined a number of parameters—the shape of meniscus, length of wire in solution, etch potential/rate, and cutoff time of etch circuit, all of which control the shape and sharpness of the end of the wire above the air/electrolyte interface. In particular, we find that the

 0734-2101/90/043570-06$01.00

cutoff time of the etch circuit has a significant effect on the radius of curvature of the etched tip; the faster the cutoff time, the sharper the tip. Therefore, an electrochemical etching circuit was designed and built with a fast cutoff time. The design and operation of the circuit is described in Sec. III. Section II reviews the electrochemical etching of tungsten.

II. ELECTROCHEMISTRY

The electrochemical etching reaction involves the anodic dissolution of tungsten in aqueous base.[29,30] The etch differs from the polishing procedures used in FIM mainly by the magnitude of the applied potential and the rate of material dissolution. Figure 1(a) shows the details of the electrochemical cell (which is similar in design to the one from W. A. Technology Ltd). It consists of a beaker containing approximately 100 ml of 2 M NaOH. The W wire is place in the center of the cell and serves as the anode. It is mounted on a micrometer so that its position relative to the surface of the electrolyte can be changed. The counter electrode (or cathode) is a piece of stainless steel shim approximately 5.5 cm wide, 13 cm long, and 25-μ thick that is cylindrically bent to fit inside the beaker around the anode at a distance of approximately 3 cm. A hole is cut into the counter electrode to permit the observation of the wire with an optical microscope during etching.

Etching occurs at the air/electrolyte interface when a positive voltage is applied to the wire (anode). The overall electrochemical reaction is:

$$\begin{array}{lll} \text{cathode} & 6H_2O + 6e^- \rightarrow 3H_2(g) + 6OH^- & \text{SRP} = -2.48\ \text{V} \\ \text{anode} & W(s) + 8OH^- \rightarrow WO_4^{2-} + 4H_2O + 6e^- & \text{SOP} = +1.05\ \text{V} \\ & W(s) + 2OH^- + 2H_2O \rightarrow WO_4^{2-} + 3H_2(g) & E^0 = -1.43\ \text{V} \end{array}, \quad (1)$$

and involves the oxidative dissolution of W to soluble tungstate (WO_4^{2-}) anions at the anode, and the reduction of water to form bubbles of hydrogen gas and OH^- ions at the cathode. E^0 is the standard electrode potential given by the sum of the standard reduction potential (SRP) for water and the standard oxidation potential (SOP) for tungsten. The tungstate anion is formed once the potential exceeds 1.43 V. It is ordinarily found, however, that the potential required to drive an electrochemical reaction is different (usually higher) than that calculated from standard electrode potentials, particularly when one of the reaction products is a gas such as hydrogen. The excess potential is required because most electrode reactions occur with an activation energy along the reaction path. This excess potential is called the electrochemical polarization. The polarization is affected by changes in the concentration of the reactants and products and other mass transfer processes; and the rate of reaction or the current density is an exponential function of the polarization.

The reaction mechanism is much more complex than indicated by Eq. (1). The actual reaction involves the oxidation of tungsten to intermediate tungsten oxides followed by the nonelectrochemical dissolution of the oxides to form the soluble tungstate anion[30] whose stability is greatest in basic medium. This reaction was found to occur over a large range of current densities and OH^- activities. In order to investigate the effect of the cell potential on the etch rate, Fig. 2 shows the potentiostatic polarization curve obtained with the electrochemical cell described above. The curves show the current–voltage (I–V) relationship for the tungsten elec-

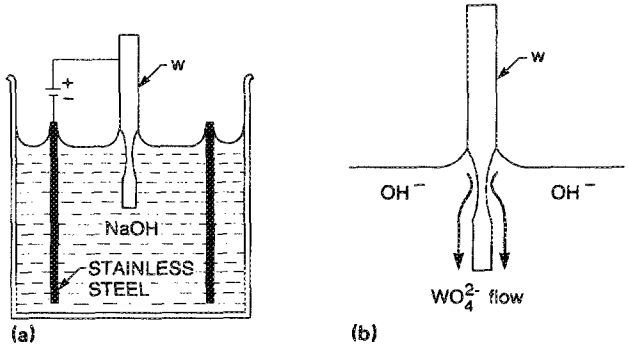

FIG. 1. (a) Schematic diagram of the electrochemical cell showing the tungsten wire (anode) being etched in NaOH. The cathode consists of a stainless steel cylinder which surrounds the anode. (b) An schematic illustration of the etching mechanism showing the "flow" of the tungstate anion down the sides of wire in solution.

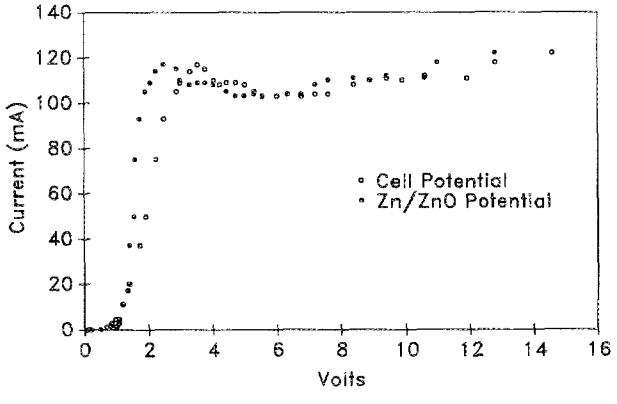

FIG. 2. Potentiostatic polarization curves for the tungsten vs (1) the applied potential of the cell (open circle) and (2) the potential at a Zn/ZnO standard electrode (closed circle). The curves show the various stages of the electrochemical reaction—on set, etching, passive film formation. The optimal etching potential for tungsten occurs over a range of 1–2 V with respect to a Zn/ZnO standard electrode. The dimensions of the tungsten wire used to obtain these curves was 20×0.25 mm in diameter.

trode versus the applied potential (open circle) or the potential at a Zn/ZnO standard electrode (a piece of Zn Wire) placed a few millimeters from the W electrode. The Zn/ZnO standard electrode removes the I–V dependence on cell geometry, size, and distance between electrodes, solution concentration/activity, etc., and allows others to apply these results to their own electrochemical cells. In our cell, the current began to rise when approximately 0.5 V (1 V versus Zn/ZnO) was applied to the W electrode. On increasing the potential, the current rose sharply reaching a plateau at approximately 4 V (2 V versus Zn/ZnO) and a current density between 0.5–0.8 A/cm.[2] Increasing the potential further (to 15 V) did not change the current density significantly, presumably due to competing reactions involving dissolution and passive film formation. Figure 2 suggests that the optimum etching potential for W dissolution should occur near 4 V (2 V versus Zn/ZnO). Increasing the potential from 0.5 to 4 V increases the rate of reaction. Above 4 V, the growth of a thick oxide film may become significant and lead to further complications with the tunneling experiment. (These results were obtained after completing the experiments described in Sec. III using the etching circuit which was designed to operate at 12 V. The results from Fig. 2 suggests that lower etching potentials should be explored as a means to control oxide formation on the tip during etching.)

The surface tension of the aqueous solution causes a meniscus to form around the wire once it is placed into the electrolyte as shown schematically in Fig. 1(b). It is primarily the shape of the meniscus which determines the aspect ratio and overall shape of the tip. The rate of etching at the top of the meniscus is much slower than at the bottom due to a concentration gradient caused by diffusion of OH^- ions to the anode. The current density of the reaction is limited by the surface area of the working electrode (tungsten) and is also dependent on the concentration and ion activity of OH^- ions.[30] The portion of the tip below the meniscus would normally be etched away if not for the flow of the denser tungstate layer down the sides of the wire, protecting the lower end. This shields the lower portion of the wire so its etch rate is less than that of the portion of the wire in the meniscus. At drop off, the lower portion of wire is still between 40%–50% of its original diameter.

The electrical resistance of the cell increases as the cross-sectional area of the wire decreases during the etch. The change in area may also cause the meniscus to drop to a lower part of the wire making it necessary to adjust the position of the wire with the micrometer. Gas bubbles sticking to the lower end of the wire should be removed as they increase the buoyancy of the wire fragment that drops off, causing the end of the tip to bend.[22]

Other parameters that affect the etch include the electrolyte concentration and the cutoff time of the etching circuit. Because OH^- is consumed in the reaction, the NaOH solution should be changed periodically. Etching times become longer as the OH^- concentration is deleted. Some typical etched times (at 12 V) for various diameter wires using a fresh NaOH solution are approximately 9, 22, and 50 min for 0.25, 0.50, and 0.75 mm diameter wires. Finally, once drop off occurs it will be important to shut off the potential as quickly as possible because any part of the wire (usually the very end of the tip) remaining in solution will continue to etch as long as there is an applied voltage. We have found that the cutoff time of the etch circuit has the most significant affect on the radius of curvature or sharpness of the tip.

III. TIP ETCHING PROCEDURE

The tips used in this study were etched in a 2 M solution of NaOH using 0.25 mm diameter tungsten wire. When the end of the wire drops off, the area of the material exposed to the electrolyte is considerably reduced causing the current density to fall. Earlier, Morgan[27] designed a circuit to supervise the electropolishing of FIM specimens. The circuit used the change in current at drop off to operate a relay that turned the circuit "off." In addition, Chen *et al.*[28] developed a technique that uses the etch current differential signal as the monitoring parameter instead of the etching current itself. We have designed and constructed an etching circuit which has a minimum cutoff time of approximately 500 ns. Figure 3 shows the circuit used to control the etch procedure; it is described in detail below.

A. Circuit control description

The circuit uses a high-speed comparator to drive two complementary metal–oxide semiconductor field effect transistors (MOSFET) in a totem pole configuration, biased at the top by + 12 V and to ground at the lower end. The components comprising the totem pole include a n-channel MOSFET field effect transistor (FET1 or Q1 in Fig. 3), a small resistor R_A which reduces current in the cutoff phase, the electrochemical etching components (indicated by a variable resistor R_{LOAD}), and a variable resistor R_B. The value of R_B determines the initial potential difference across the load V_{LOAD} by the following equations:

$$I_{\mathrm{LOAD}} = 12\mathrm{V}/(R_{\mathrm{ON}}\{\mathrm{FET1}\} + R_A + R_{\mathrm{LOAD}} + R_B), \tag{2}$$

$$V_{\mathrm{LOAD}} = V_A - B_B = I_{\mathrm{LOAD}} \times R_{\mathrm{LOAD}}. \tag{3}$$

Typical values for the variables in the above equations are: $R_{\mathrm{ON}}\{\mathrm{FET1}\} \approx 1.5\Omega, R_A \approx 50\Omega$, and R_{LOAD} starts at about 200–400 Ω, depending on the length of the wire in solution. The variable resistor R_B has a great effect on the potential across the load; the smaller its resistance, the higher the potential (and vice versa). Voltage V_B is applied to the inverting input of the LM306 comparator, and is compared to a reference voltage V_{REF} which is generated by a voltage divider that uses a 10 KΩ multiturn potentiometer for the accurate setting of low cutoff voltages.

The comparator integrated circuit (IC) is a 40 ns response time device which is powered by ± 12 V with a 2.2 KΩ pull-up resistor across its open-collector output, allowing outputs of 0 or 12 V. The output voltage (V_{OUT}) is connected directly to the gates of the two MOSFET transistors, which have a low on-state resistance (1.5–4.5 Ω) and 15 ns switching time. Also connected to the output (not shown) is a window discriminator circuit which turns on either a green or red light emitting diode (LED), depending on whether the cir-

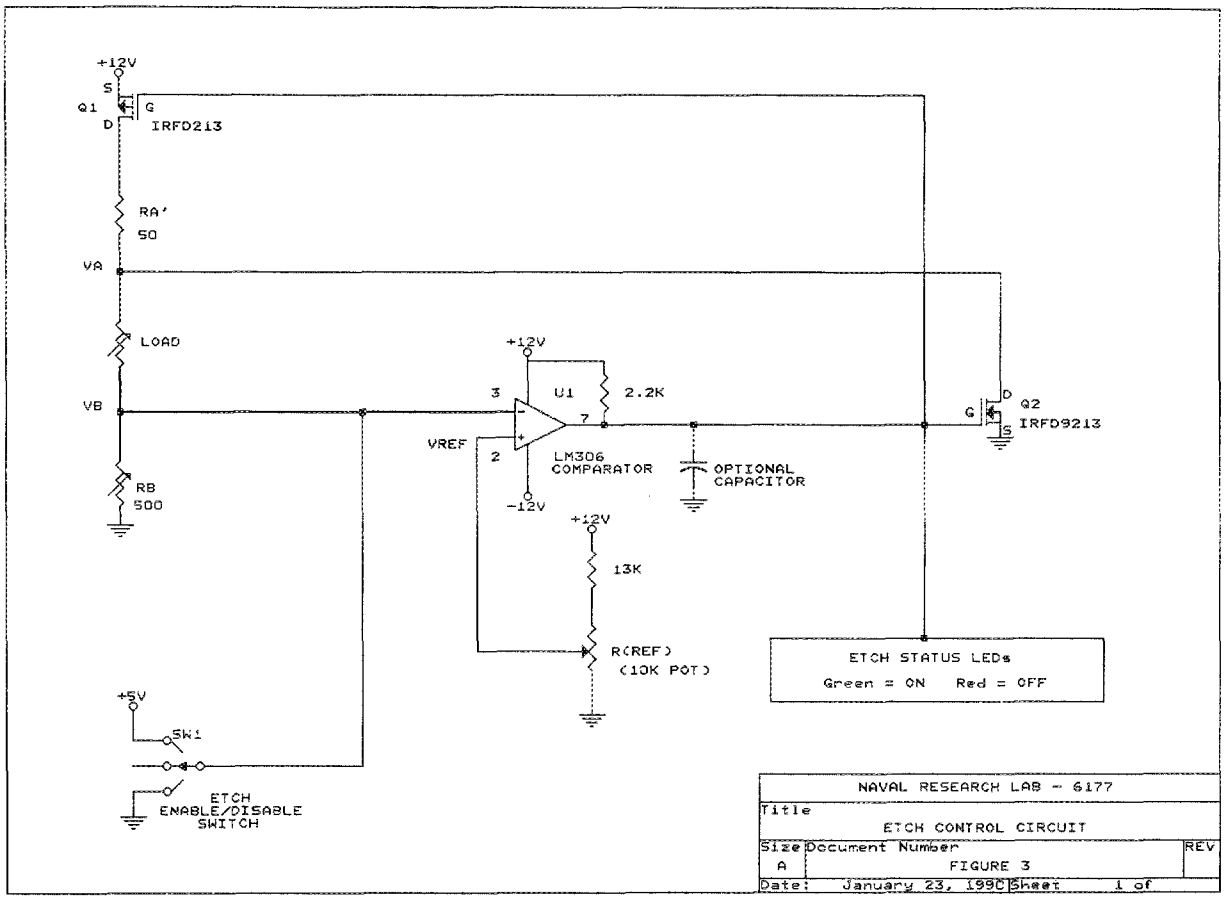

FIG. 3. The electronic control circuit designed to minimize the electrochemical reaction cutoff time following drop-off. R_{LOAD} denotes the electrochemical cell.

cuit is on or off. Optionally, a capacitor can be placed across V_{OUT} to slow down the response time of the comparator, resulting in an increased switching time for the circuit.

When the output of the comparator (V_{OUT}) is low, the gate terminals of both transistors are at approximately ground. This biasing puts FET1 into its region of conductance (V_{GS1} less than -4 V) and turns off FET2 (V_{GS2} less than 4 V). Since FET2 (Q2 in Fig. 3) is off, no current is shunted away from the etch. This mode of operation represents the "ON" state of the etch, and is the case when V_B is greater than V_{REF}, indicated by the green LED. As the etch progresses, the value of R_{LOAD} increases causing a proportional increase in potential across the load, reducing the voltage V_B. When V_B drops below V_{REF}, V_{OUT} switches from low to high. At V_{OUT} equal to approximately 4 V, FET2 turns on and begins to shunt current away from the load. At V_{OUT} equal to approximately 8 V, FET1 reaches its gate-source cutoff voltage, reducing the drain current to near zero and turning the transistor off. This mode of operation is the "OFF" state of the etch, indicated by the red LED. To insure proper starting of the etch process, a manual etch enable/disable switch was installed. Toggling the switch up sends $+5$ V into V_B starting the etch process; while toggling it down brings V_B to ground turning off FET1 and stopping the etch.

It is important to set V_{REF} close to the drop-off voltage. Setting V_{REF} too high will result in a premature shut-off of the circuit (not a bad result); while setting it too low will result in some back etching, dulling the tip. Although it is difficult to know in advance the *exact* drop-off voltage, using the same amount of wire in solution should keep the drop-off voltage relatively constant. Placing approximately 2 mm of the 0.25 mm diam wire gives a drop-off voltage of 130–160 mV. For these experiments, a V_{REF} of 145 mV was used.

B. Cutoff time

R_{LOAD} increases as more and more of the tungsten wire is etched away due to a decrease in cross-sectional area. Eventually, the weight of the stub exceeds the tensile strength of the etched wire causing it to drop off into the solution. At this point there is a sudden change in resistance from about 1 KΩ to several MΩ, which appears as a sharp drop in the voltage V_B. A LeCroy model 9400 125-MHz digital oscilloscope was used to measure V_B as a function of time in order to establish the cutoff time for the etch. The cutoff time is defined as the time that it takes V_B to drop to (or below) ground potential. As noted in the circuit description, a capacitor can be attached across the output to slow down the switching time of the circuit, resulting in an increase of the etch cutoff time. The capacitor and pull-up resistor create a resistance-capacitance (RC) circuit that delays the output voltage and causes the tip to be etched after the stub has

dropped off, thus dulling the point. Table I summarizes the data showing the change in cutoff time for the etch with different capacitors. Increasing the time constant of the circuit increases the cutoff time of the etch.

A noteworthy feature of this circuit is that its ON-to-OFF switching operation represents positive feedback which tends to speed-up the switching from one stable state to another. Even though the circuit uses ultrafast components, cutoff time of 500 ns is relatively slow and is probably due to the way that we drive the circuit. When the comparator switches to turn off the etch, it changes from a low impedance state to a high impedance state, thus requiring the pull-up resistor. A faster circuit could be made possibly by using the low impedance state of the comparator to stop the etch.

IV. RESULTS AND DISCUSSION

A. Sharpness of tips

Figure 4 shows the corresponding scanning electron micrographs of the tips whose cutoff times are given in Table I. The photos in each column have the same magnification. The scale marker corresponds to 100 and 1.0 μm in the left and right-hand columns, respectively. The approximate radii of curvature (ROC) for the tips shown in Figs. 4(a), 4(b), and 4(c) are 20, 50, and 87 nm, respectively. The corresponding cone angles measured at 100 000× magnification are 10°, 42°, and 60°, respectively. After etching over 50 tips, we find an average ROC of 32 ± 16 nm and cone angles of 10° ± 3° for tips etched with a 600 ns cutoff time, 58 ± 30 nm and 37° ± 8° for tips etched with a 150 ms cutoff time, and 100 ± 30 nm and 52° ± 11° for tips etched with a 640 ms cutoff time.

B. Length of wire in solution

Another etch parameter that was varied in our experiment was the length of wire in solution. It was found that the length of wire in solution has a direct effect on the tip, with longer lengths causing the stub to drop off much sooner due to the increased weight. Since the drop off occurs when less of the wire has been etched away, these tips have a correspondingly larger radius of curvature than those of a shorter length (e.g., 110 nm for wires with 4 mm of length in solution and 230 nm for wires with 6 mm of length in solution compared to 32 nm for wires with 2 mm of length in solution). In our trials, lengths from 1–15 mm were tested. For the 0.25 mm diam wire, lengths in the range of 1–3 mm consistently gave tips with the smallest radii of curvature.

It was also noted that many of these tips had a ball-like

TABLE I. Summary of data relating the circuit time constant to etch cutoff time, tip radius of curvature (ROC) and cone angle.

RC capacitor (μF)	Etch cutoff time (ms)	Tip ROC (nm)	Cone angle[a] (degrees)
none	0.0006	32 ± 16	10 ± 3
150	140	58 ± 30	37 ± 8
600	640	100 ± 30	52 ± 11

[a] Measured at 100 000× magnification.

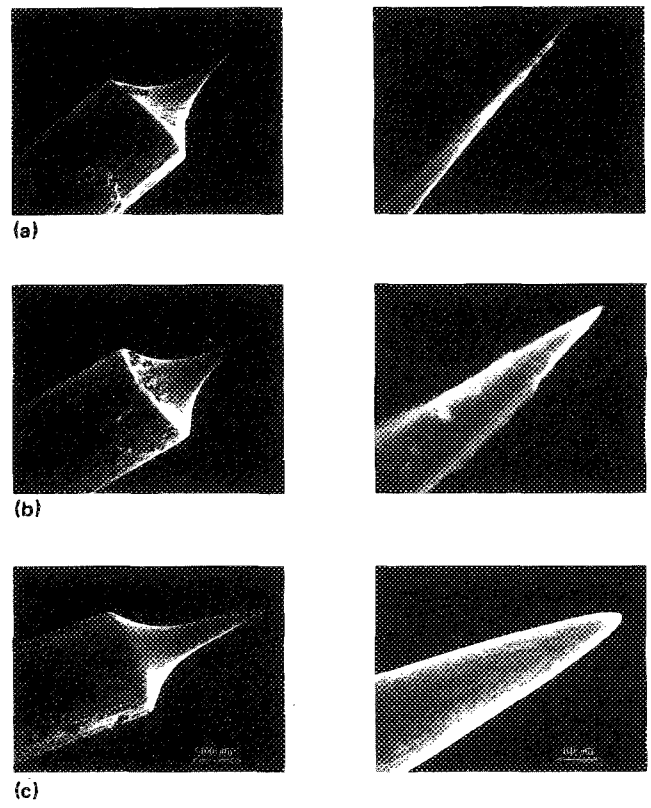

FIG. 4. Scanning electron micrographs of tips whose electrochemical etch cut-off times are (a) 600 ns, (b) 140 ms, and (c) 640 ms. The photos in each column have the same magnifications. The feature size is indicated by the scale markers.

structure at the very end of the tip increasing the effective radius of curvature. During the etch there are two forces acting on the wire: the weight of the stub pulling down on the wire and the wire pulling up on the stub. As long as the downward force does not exceed the tensile strength of the neck, it will not break. However, when the weight exceeds this strength, the stub breaks off removing the downward force on the wire. As a result, the material at the end of the tip may experience a slight recoil and bend the tip, or the energy release may be high enough to cause local "melting" when the stub drops off causing the ball to form. This phenomenon occurs more frequently as the length of the wire in solution is increased, and hence the weight of the stub is increased.[31] For the 0.5 mm diameter wire, more than 4 mm of wire in solution seems to produce the ball shape; whereas for the 0.25 mm wire, it occurs for lengths of 3 mm or greater. Therefore, we anticipate that methods which produce relatively long drop-off portions or which hang a weight to the end of the wire below the air–electrolyte interface to promote fracture will produce tips with much larger radii of curvature.

C. Tip/meniscus shape

Another variable which can affect the shape of the tip is the height and shape of the meniscus. The meniscus height starts out at a certain level, but during the etch it may fall due to a variety of reasons including fluid disturbances and the changes in surface area of the wire as it is etched. To avoid

oddly shaped tips, the meniscus height is generally brought back to its original position by adjusting the micrometer. In addition, there is usually some "play" in height at which the meniscus can be adjusted. For example, moving the wire in the direction away from the air/electrolyte interface tends to stretch the meniscus. Moving the tip in the opposite direction shortens the meniscus height. The height of the meniscus directly affects the aspect ratio; the shorter the meniscus, the smaller the aspect ratio. A low aspect ratio is important in reducing vibration in the tip.

V. CONCLUSIONS

In this work, we have investigated a number of parameters—shape of the meniscus, length of wire in solution, etch voltage, and etch cutoff time—which affect the shape and sharpness of the portion of wire that remains above the air/electrolyte interface following dc drop off. While the study focuses on the anodic dissolution of tungsten wire in NaOH, we believe that the results are generally applicable to other metals. We find the etch circuit cutoff time to have the most significant effect on the sharpness of the tip; the faster the cutoff time, the sharper the tip. We have designed and built an etching circuit which has a minimum cutoff time of 500 ns. We have demonstrated that the faster cutoff time gives small ROC tips with smaller cone angles. The etching circuit presently operates at a potential of 12 V; however, the results from the potentiostatic polarization measurement suggest that etching at lower voltages may also be beneficial.

ACKNOWLEDGMENTS

The authors would like to thank our Naval Research Laboratory colleagues Bill O'Grady and Graham Cheek for helpful discussions concerning the electrochemistry. Special thanks goes to Michael Weimer and Bob Driscoll who introduced one of us (R. J. C.) to the problems (and solutions!) of tip etching during a sabbatical at Caltech. Funding support from the Office of Naval Research is gratefully acknowledged. This work was done while S. L. B., R. A. B., and N. A. B. held National Research Council–Naval Research Laboratory Associateships.

[a] Geo-Centers, Inc., Ft. Washington, MD 20744.
[b] Sachs–Freeman Associates, Inc. Landover, MD 20785.
[c] Surface Physics Branch, Code 6831.

[1] G. Binnig, H. Rohrer, Ch. Gerber, and E. Weibel, Phys. Rev. Lett. **49**, 57 (1982).
[2] G. Binnig and H. Rohrer, Helv. Phys. Acta **55**, 726 (1982).
[3] J. Tersoff and D. R. Hamann, Phys. Rev. Lett. **50**, 1998 (1983); Phys. Rev. B **31**, 805 (1985).
[4] E. Stoll, Surf. Sci. **143**, L411 (1984).
[5] Y. Kuk, P. J. Silverman, and H. Q. Nguyen, J. Vac. Sci. Technol. A **6**, 524 (1988).
[6] G. W. Stupian and M. S. Leing, Rev. Sci. Instrum. **60**, 181 (1989).
[7] P. K. Hansma and J. Tersoff, J. Appl. Phys. **61**, R1 (1987).
[8] J. A. Stroscio, R. M. Feenstra, and A. P. Fein, Phys. Rev. Lett. **58**, 1668 (1987).
[9] H. Neddermeyer and M. Drechsler, J. Microsc. **152**, 459 (1988).
[10] V. T. Binh, J. Microsc. **152**, 355 (1988).
[11] D. K. Biegelsen, F. A. Ponce, J. C. Tramontana, and S. M. Koch, Appl. Phys. Lett. **50**, 696 (1987).
[12] D. K. Biegelsen, F. A. Ponce, and J. C. Tramontana, Appl. Phys. Lett. **54**, 1223 (1989).
[13] R. Guckenberger, C. Kösslinger, R. Gatz, H. Breu, N. Levai, and W. Baumeister, Ultramicroscopy **25**, 111 (1988).
[14] P. J. Bryant, H. S. Kim, Y. C. Zheng, and R. Lang, Rev. Sci. Instrum. **58**, 1115 (1987).
[15] M. J. Heben, M. M. Dovek, N. S. Lewis, R. M. Penner, and C. F. Quate, J. Microsc. **152**, 651 (1988).
[16] L. A. Nagahara, T. Thundat, and S. M. Lindsay, Rev. Sci. Instrum. **60**, 3128 (1989).
[17] H-W. Fink, IBM J. Res. Dev. **30**, 460 (1986).
[18] Y. Kuk and P. J. Silverman, Appl. Phys. Lett. **48**, 1597 (1986).
[19] Y. Kuk, P. J. Silverman, and H. Q. Nguyen, J. Vac. Sci. Technol. A **6**, 524 (1988).
[20] V. T. Binh and J. Marien, Surf Sci. **202**, L539 (1988).
[21] T. Hasizume, I. Kamiya, Y. Hasegawa, N. Sano, T. Sakurai, and H. W. Pickering, J. Microsc. **152**, 347 (1988).
[22] E. W. Müller and T. T. Tsong, *Field Ion Microscopy* (Elsevier, New York, 1969), pp. 119–23.
[23] K. M. Bowkett and D. A. Smith, *Field Ion Microscopy* (Elsevier, New York, 1969), pp. 57–60.
[24] A. J. Melmed and J. J. Carroll, J. Vac, Sci. Technol. A **2**, 1388 (1984).
[25] H. Morikawa and K. Goto, Rev. Sci. Instrum. **59**, 2159 (1988).
[26] J. L. Watkins, NASA Tech Briefs, May/June 1986, p. 135.
[27] R. Morgan, J. Sci. Instrum. **4**, 808 (1967).
[28] Y. Chen, W. Xu, and J. Huang, J. Phys. E **22**, 455 (1989).
[29] J. W. Johnson and C. L. Wu, J. Electrochem. Soc. **118**, 1909 (1971).
[30] G. S. Kelsey, J. Electrochem. Soc. **124**, 814 (1977).
[31] R. Nicolaides, Y. Liang, W. E. Packard, Z.-W. Fu, H. A. Blackstead, K. K. Chin, J. D. Dow, J. K. Furdyna, W. M. Hu, R. C. Jaklevic, W. J. Kaiser, A. R. Pelton, M. V. Zeller, and J. Bellina, J. Vac. Sci. Technol. A **6**, 445 (1988).